Bridging the Green Gap: Metal–Organic Framework Heteromultilayers Assembled from Porphyrinic Linkers Identified by Using Computational Screening

Haldar, R.; Batra, K.; Marschner, S. M.; Kuc, A. B.; Zahn, S.; Fischer, R. A.; Bräse, S.; Heine, T.; Wöll, C.;

Bridging the green gap: MOF hetero-multilayers assembled from porphyrinic linkers identified using computational screening

Ritesh Haldar,±[a] Kamal Batra,±[b] Stefan Michael Marschner,[c] Agnieszka B. Kuc,[d] Stefan Zahn,[e] Roland A Fischer,[f] Stefan Bräse,[c,g] Thomas Heine,*[b,d] Christof Wöll*[a]

Abstract: In organic photovoltaics, porphyrins (PPs) are among the most promising compounds owing to their large absorption cross section, wide spectral range, and stability. Nevertheless, a precise adjustment of absorption band positions to reach a full coverage of the so-called green gap has not been achieved yet. We demonstrate that a tuning of the PP Q- and the Soret bands can be done using a computational approach where substitution patterns are optimized in silico. The Most promising candidate structures were then synthesized. The experimental UV/Vis data for the solvated compounds were in excellent agreement with the theoretical predictions. By attaching further functionalities, which allow using the PP chromophores as linkers for the assembly of metal-organic frameworks (MOFs), we were additionally able to exploit packing effects resulting in pronounced red shifts, which allowed to further optimizing the photophysical properties of PP assemblies. Finally, we use a layer-by-layer method to assemble the PP linkers into surface-mounted MOFs (SURMOFs), thus obtaining high optical quality, homogeneous and crystalline multilayer films. Experimental results are in full accord with the calculations, demonstrating a huge potential of computational screening methods in the tailoring of MOF

[a]   Dr. R. Haldar, Prof. Dr. C. Wöll
        Karlsruhe Institute of Technology (KIT)
        Institute of Functional Interfaces (IFG)
        Hermann-von-Helmholtz Platz 1
        76344 Eggenstein-Leopoldshafen (Germany)
        E-mail: christof.woell@kit.edu
[b]   K. Batra, Prof. Dr. T. Heine
        Theoretische Chemie, Technische Universität Dresden
        Bergstraße 66c, König-Bau
        01062 Dresden (Germany)
        E-mail: thomas.heine@tu-dresden.de
[c]   S. M. Marschner, Prof. Dr. S. Bräse
        Karlsruhe Institute of Technology (KIT)
        Institute of Organic Chemistry (IOC)
        Fritz Haber Weg 6
        76351 Karlsruhe (Germany)
[d]   Dr. A. B. Kuc, Prof. Dr. T. Heine
        Helmholtz-Zentrum Dresden-Rossendorf
        Permoserstraße 15
        04318 Leipzig (Germany)
[e]   Dr. S. Zahn
        Leibniz Institute für Oberflächenmodifizierung e.V.
        Permoserstraße 15
        04318 Leipzig (Germany)
[f]   Prof. Dr. R. A. Fischer
        Technical University of Munich
        Lichtenberg Straße 4
        85748 Garching (Germany)
[g]   Prof. Dr. S. Bräse
        Karlsruhe Institute of Technology (KIT)
        Institute of Toxicology and Genetics (ITG)
        Hermann-von-Helmholtz Platz 1
        76344 Eggenstein-Leopoldshafen (Germany)
        ± Authors contributed equally.

        Supporting information for this article is given via a link at the end of the document.((Please delete this text if not appropriate))

and SURMOF photophysical properties.

While presently the highest conversion efficiencies are achieved with inorganic (Si, Ge)[1] and hybrid (Grätzel-cell, perovskites)[2] semi-conductor based photovoltaic (PV) devices, organic materials are an interesting alternative with advantages in more specific applications.[3] Main obstacles in this area are efficiency and stability issues. Progress in this field is only gradual, and the search for organic molecules suited as an active PV material is to a large extent still dominated by empirical approaches.[3,4] Use of computer-based screening methods is hampered by the fact that the characteristics of most organic PV (OPV) materials are strongly impacted by intermolecular interactions.[5] and, for disordered systems, many configurations have to be samples to make reliable predictions.[6]

Major progress has thus to be expected when employing crystalline systems with exactly known structures.[7] In such cases, periodic boundary conditions can be applied, which allows for a thorough theoretical analysis utilizing the solid state analysis toolbox.[6] The OPV device characteristics can then be predicted on the basis of first-principles electronic structure calculations carried out both for single molecules as well as for the condensed phases of these organic semiconductors. In the latter case, the precise arrangement of the functional molecules in the crystalline state is taken fully in account. In addition to a reliable theoretical analysis with high predictive power, for crystalline systems additional effects may be employed, e.g. the emergence of band dispersion favoring large charge carrier mobilities and the formation of indirect band gaps.[8] Indirect band gaps are beneficial in photovoltaics since they favor a fast and highly efficient charge separation and thus charge carrier recombination is strongly suppressed.

Here, we demonstrate an approach based on assembly of multi-functionalized PP linkers into thin films of MOFs.[9] PPs are a particular promising class of organic compounds for investigating the beneficial effect of a regular arrangement of photoactive molecules with regard to light harvesting.[10] PPs form a very rich class (> 100,000 compounds known)[11,12] which are also common in nature. In plants, PPs like chlorophyll transform solar energy into chemical energy. Since PPs are among the best-performing organic compounds regarding photon absorption, charge separation, and stability,[12] numerous previous works have been carried out with the aim to prepare well-defined, thin films of PP aggregates deposited on conducting and transparent substrates.[13] The approaches employed previously include vapour-phase deposition of PP molecules, a rather sophisticated method, or self-assembly from appropriate solutions. The latter strategy has been rather successful, but the resulting systems do not exhibit a high degree of ordering, thus largely excluding the formation of band-structure effects. In addition, the different types of molecular
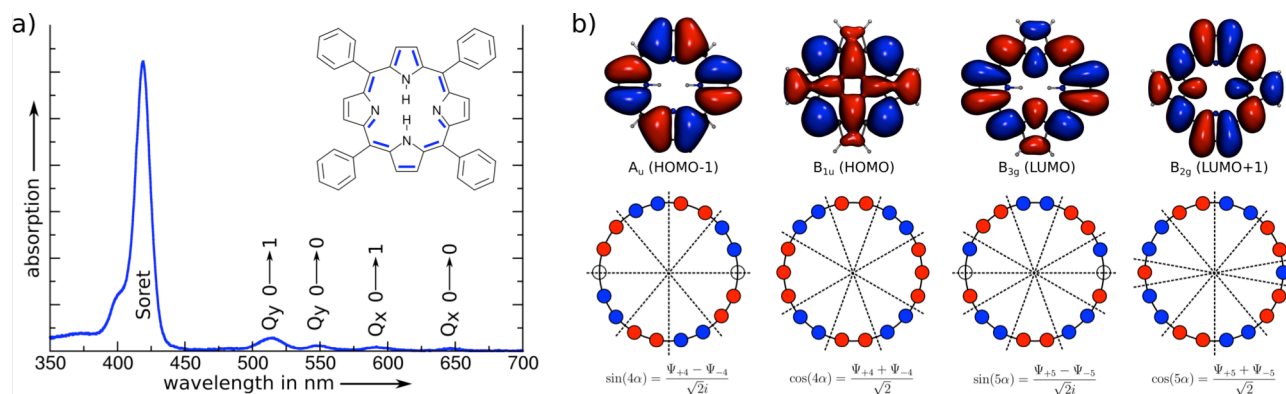
Figure 1. a) Typical spectra of a porphyrin. Blue lines in the Lewis structure highlight the π-electrons on which a 18π cyclic polyene model is reasonable; b) Comparison of the frontier orbitals obtained from DFT calculations of porphyrin and the 18π cyclic polyene model.

packing in the amorphous films make more precise predictions of absorption properties difficult.

The typical absorption spectrum of a PP chromophore consists of a sharp, high-intensity Soret band, which is typically located in the UV region, and four Q bands located in the visible range (Figure 1a). In principle all transitions of the frontier orbitals are symmetry-allowed. However, as the frontier orbitals are nearly degenerate, the electronic structure can be approximated by a 18 π cyclic polyene model, as suggested by Gouterman,[14] where two transitions are allowed between the degenerated frontier orbitals (Δk=1), while two are forbidden (Δk=9) (Figure 1b). Detailed quantum chemical studies confirm Gouterman's conclusions and explain the typical absorption spectra of PPs in detail.[15] Tuning the energy levels of HOMO-1, HOMO, LUMO and LUMO+1 strongly affects the absorption intensity of the characteristic absorption bands of porphyrins. The higher the energy gap between HOMO-1 and HOMO as well as LUMO and LUMO+1, the stronger will be the absorption intensity of the Q-bands. While this allows the rational design of PP molecules, the prognostication of absorption spectra for PP-based SURMOFs remains difficult. This is mainly due to the fact that the bulk structure is not known a priori, and changes of absorption intensity and band positions resulting from intermolecular interactions are thus difficult to predict.

Here, we circumvent the problem of structure prediction for the condensed phase by focusing on porphyrinic dicarboxylic acids which can be used as ditopic linkers to assemble PP-MOFs. In order to identify a small set of chromophoric MOF linkers to cover the green gap we first carried out a computational screening of a library containing 14 PP structures (Figure S1). This library was generated by functionalization of two of the phenyl rings at the *meso* positions with carboxylate groups to produce ditopic MOF linkers. In the first group of PP derivatives, the H atoms at the β positions are substituted by halides and methyl groups (**1**-X group, X = F, Cl, Br, CH$_3$), and in the second group the two phenyl rings that do not serve as linking groups are substituted. The library contains substitution groups which can modulate PP ring planarity (e.g. substitution at β-position by bulky Br atoms), and also electron density (electron donating /pulling).

In order to obtain theoretical predictions with sufficient reliability, simplified time-dependent density-functional theory (sTD-DFT) was applied (see SI for computational details). As expected, functionalization is found to be a suitable means for both Q band intensity enhancement and tuning of absorption band positions. For example, β substitution by Br as well as *meso* positioned phenyl group substitution creates a large red shifts of Q bands by >50 nm in comparison to **1-H** (see Table
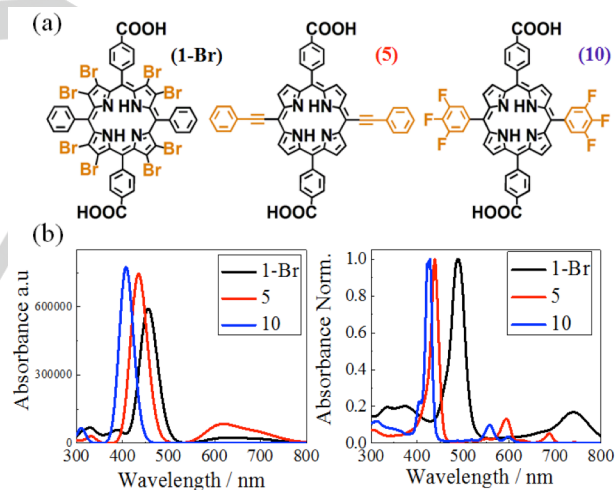

Figure 2. a) Three selected PP linkers; (b) TD-DFT predicted (left) and experimental (right) UV-Vis spectra of the linkers. Experimental spectra were recorded for 20 μM ethanolic solution of the linkers at RT.

S2). Additionally, the absorption of the Q bands is significantly enhanced (Figure S3).

On the basis of this computational screening, three PPs (Figure 2a) have been selected for synthesis (see experimental section in supporting information) and validation of the theoretical predictions. Selection criteria were the enhancement of Q-band intensity and the tuning of band position. These selected three PPs exhibit important differences: i) the presence of electron withdrawing functional groups (fluorinated phenyl), ii) π- conjugation of the substituent (phenyl group or acetylene

group), and iii) planarity of the porphyrin core (twisted octabromo porphyrin). The experimental methods developed for organic synthesis of the multi-substituted porphyrins were successful. The required A2B2-type porphyrins were assembled in a modular fashion starting from dipyrromethene building blocks and functional aldehydes. Subsequent cross-coupling reactions led to the designed porphyrins (see experimental section in supporting information). Figure 2b, shows the predicted (left) and experimental (right) UV-Vis spectra of **1-Br, 5** and **10**. Generally, a good agreement is seen between the TD-DFT gas-phase predictions and the experimental results (solvated). Note, that the agreement is not expected to be quantitative since solvatochromic shift affect the experimental absorption spectra.[16] In these synthesized PPs, apart from the Q-bands in near-IR region, also the Soret band shifts to visible range, in comparison to the **1-H**.

For applications, the assembly of PP dyes into thin films of high optical quality is crucial. Therefore, in a final step, the selected PP linkers were assembled into SURMOF-2 thin films containing optically silent Zn_2 paddle wheel units, following the spin-coated variant of the layer-by-layer (lbl) liquid phase epitaxy method.[17] The SURMOF-2 structure consists of Zn_2-paddle-wheel (PW) type secondary building units (SBUs) tethered with
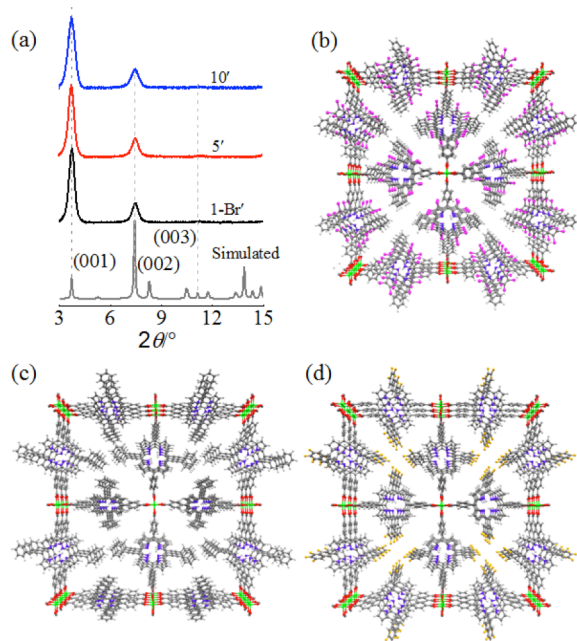

Figure 3. a) Simulated XRD pattern of **1-Br′**, and experimental out-of-plane XRD patterns of **1-Br′**, **5′** and **10′**; calculated atomistic structures of b) **1-Br′**, c) **5′** and d) **10′**, view along [010] direction.

ditopic linkers to yield two-dimensional planes stacked along the (010) crystallographic direction (Figure 3).[18] Note that the framework of SURMOF-2 has *P*4 symmetry, and the lattice constant only depends on the length of the PP linkers (i.e. the distance between the two carboxylic acid groups), while the addition of side-groups to the PPs are not expected to create changes of the SURMOF unit cell.

In all three cases, SURMOF-2 structures, labelled as **1-Br′**, **5′** and **10′**, exhibit well-defined out-of-plane XRD patterns

(Figure 3a). The position of the diffraction peaks are almost identical, yielding unit cell dimensions with *a* = *b* = 2.3 nm, in excellent agreement with the prediction. These observations confirm the expectation that irrespective of the type of group attached at *meso* or β position to the PPs, the unit cell parameters of the resulting MOF structures remain unchanged. (Figure 3, for details, see supplementary information). Figures 3b-d show the DFTB optimized atomistic structures of **1-Br′**, **5′** and **10′**. In **10**, fluorination of the linkers creates significant electrostatic repulsion, so the inter-linker distance is maximized
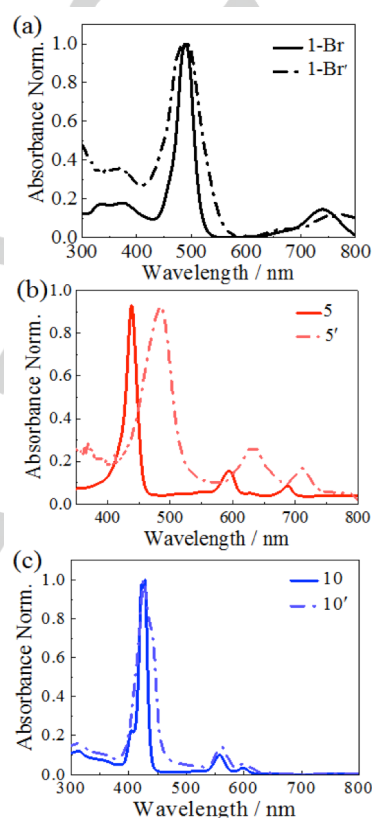

Figure 4. Experimental UV-Vis comparison spectra of the synthesized PP linkers (solid line) and their corresponding fabricated SURMOF-2 structures (broken line); a) **1-Br**, b) **5** and c) **10**. Note that the molecular spectra are recorded in ethanol at RT.

when the PPs are untwisted. This maintains the overall *P*4 symmetry in **10** with a distance between the PP units of 6.3 Å. In contrast, the longer linkers in **5′** interact strongly, causing a tilting of 34° and reducing the distance between the PP planes to 3.6 Å. these of the solvated linker molecules **1-Br**, **5** and **10**. In **1-Br′**,

Figure 4 compares the UV-Vis spectra of **1-Br′**, **5′** and **10′** with the distorted basal planes of the linker (**1-Br**) prevent periodicity along the PP stacks (along (010)). Consequently, the bands are not shifted compared to those of the solvated **1-Br**, but significantly broadened (Figure 4a). However, the experimental data reveal that crystallization of **5** in the SURMOF-2 structure causes a significant red shift of all bands in **5′** (Figure 4b). Notably, this red shift affects both the Soret and the Q bands. In addition, all bands are substantially broadened. The spectra of **10** and **10′** are very similar, indicating

negligible interaction between the PP linkers (also in line with the predicted structure) (Figure 4c).

To rationalize the experimental UV-Vis spectra recorded for the PP-SURMOFs, we have calculated the band structures of **1-Br′**, **5′** and **10′** (for details, see supporting information), which are shown in Figure 5(a-c). The band structure of **1-Br′** reflects the idealized structure and therefore is not directly suitable to interpret the UV-Vis spectrum (Figure 5a). For **5′**, we observe significant band dispersion along the Z direction of the Brillouin zone (see Figure 5b, 5d), which is responsible, both for the red shift of the absorption bands, as well as for the charge carrier mobility along the PP stacks (along (010)). We observe an indirect band gap of ~ 200 meV, which is substantially larger than that (5 meV) reported in previous work for a different PP-SURMOF-2 structure.[19] Note, that for steric reasons in the single unit cell approach only one stack of linkers is tilted in our atomistic structures, which is reflected in the presence of only one dispersed valence and one dispersed conduction band. For **10′**, no band dispersion is observed, confirming the hypothesis that the linker molecules **10** do not interact in the SURMOF-2 structure (Figure 5c). As a result, the UV-Vis data for the corresponding SURMOF-2 film mainly show the molecular features. Due to the lack of band dispersion, no ballistic transport is possible for such structure. While for the **1-Br′** and **10′** no substantial aggregation-induced shifts of the absorption band positions were observed, a broadening of the absorption bands is evident. This is a beneficial effect, and together the three PP-linkers allow covering the full visible spectrum ranging from violet to near-IR. Inspired by such broad absorption, we have fabricated a multilayer SURMOF-2 structure by employing heteroepitaxy.[20] Layers of **1-Br′**, **5′** and **10′** were sequentially deposited on top of each other to make a crystalline thin film with a broad absorption ranging UV-to-NIR, as shown in Figure 5e. Such straightforward fabrication method, combining all the potential photon absorbing dyes as a thin film is a promising strategy towards further improvement of OPV materials.

In conclusion, we present here an attractive route to create OPV absorber layers in the visible regime, covering the entire range from the violet to the near infrared, including the green gap. Starting point is a set of candidate structures, in this case, tetraphenyl porphyrin derivatives with different substitution patterns. Instead of scheduling a vast amount of structures for synthesis, we used a computational approach to first select promising chromophoric MOF linkers from an *in-silico* library. Indeed, after synthesis, the three candidates, showed excellent performance. **1-Br** exhibits distorted basal plane that imposes a significant red shift of both Soret and Q-bands in the free molecule. The second one (**5**) has a large aromatic ligand (extended conjugation), which enhances the Q-band intensity, but does not affect the position of the Soret band. The third one (**10**) is functionalized with strong electrostatically active groups. Arranging these dyes into a SURMOF-2 structure yields three different pictures: In **1-Br′**, distorted basal planes of the linkers avoid regular stacking, and while the positions of the absorption bands of the free linkers are maintained, they are significantly broadened in the SURMOF structure. In **5′**, the strong intermolecular interactions lead to a red shift and broadening of all bands. Finally, in **10′**, electrostatic repulsion reduces intermolecular interactions and thus the absorption spectrum of
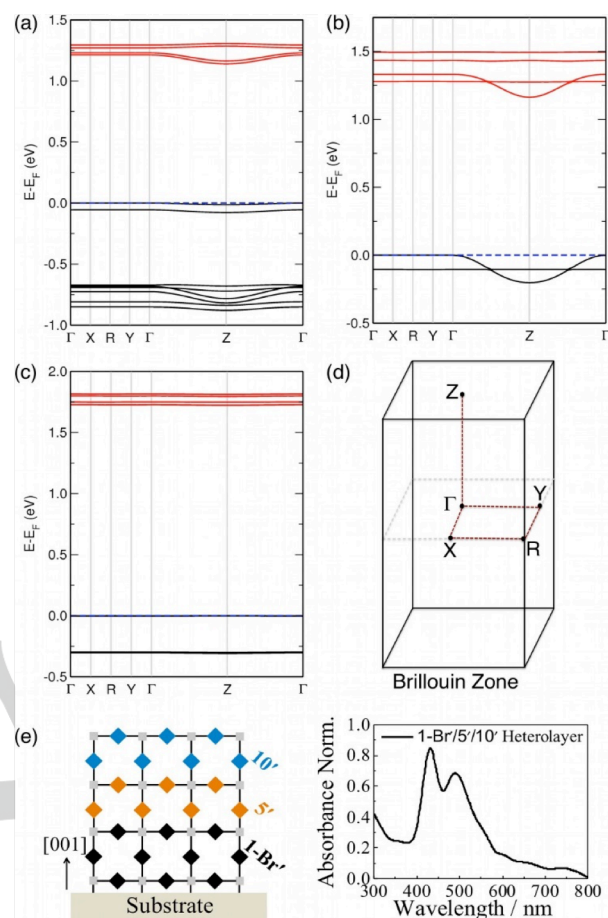

Figure 5. (a-c) Band structure of **1-Br**, **5′** and **10′**; (d) brillouin zone; (e) a schematic illustration of trilayer SURMOF (left) and corresponding UV-Vis spectrum (right). (The gray filled box = SBU, filled diamond shape = PP).

the corresponding SURMOF is dominated by the molecular properties of **10**.

Altogether our results reveal that the strategy to prepare chromophoric assemblies via a SURMOF-based approach carries a huge potential. Depending on the stacking within the MOF, one can realize systems with small inter-chromophore coupling, which are essentially dominated by features of the individual molecules. By adjusting the MOF topology together with chromophore substitution patterns, intermolecular couplings can be introduced, which allow to invoke band structure effects, thus increasing charge carrier mobility and allowing of indirect band gap formation. Finally, the SURMOF approach then provides the prospect to realize energy funneling via fabrication of hetero-multilayers or gradient structures.

Experimental Section

Fabrication of SURMOFs: Ethanolic solution of 1 mM zinc acetate and 20 µM porphyrin linker solutions (in Ethanol) were sequentially deposited onto the substrates using spin coating method in a layer-by-layer fashion. After the metal or linker coating, the samples were rinsed with ethanol to

remove unreacted metal/linker or by-products from the surface. For metal and linker both, the spin coating time is fixed as 10 s with rpm of 2000. The thickness of the samples was controlled by the number of deposition cycles. In a similar fashion, multilayer SURMOF-2 was fabricated. Each of the PP linkers (**1-Br**, **5** and **10**) were deposited for 25 cycles. Details on synthesis of molecular compounds and computational details are given in the SI.

[1]   a) F.-J. Haug, C. Ballif, *Energy Environ Sci.* **2015**, *8*, 824-837; b) P. Gao, Z. Yang, J. He, J. Yu, P. Liu, J. Zhu, Z. Ge, J. Ye, *Adv. Sci.* **2018**, *5*, 1700547.

[2]   a) F. Bella, C. Gerbaldi, C. Barolo, M. Grätzel, *Chem. Soc. Rev.* **2015**, *44*, 3431-3473; b) L. M. Peter, *J. Phys. Chem. Lett.* **2011**, *2*, 1861-1867; c) D. Yang, R. Yang, S. Priya, S. Liu, *Angew. Chem. Int. Ed.* **2019**, 58, DOI: 10.1002/anie.201809781; d) Z. Li, T. R. Klein, D. H. Kim, M. Yang, J. J. Berry, M. A. F. M. van Hest, K. Zhu, *Nat. Rev. Mater.* **2018**, *3*, 18017.

[3]   a) P. Cheng, X. Zhan, *Chem. Soc. Rev.* **2016**, *45*, 2544-2582; b) D. M. Stolzfus, J. E. Donaghey, A. Armin, P. E. Shaw, P. L. Burn, P. Meredith, *Chem. Rev.* **2016**, *116*, 12920-12955.

[4]   a) G. Wang, F. S. Melkonyan, A. Facchetti, T. J. Marks, *Angew. Chem. Int. Ed.* **2019**, *58*, DOI: 10.1002/anie.201808976 b) W. Xu, F. Gao, *Mater. Horiz.* **2018**, *5*, 206-221.

[5]   K.-H. Kim, H. Yu, H. Kang, D. J. Kang, C.-H. Cho, J. H. Oh, B. J. Kim, *J. Mater. Chem. A.* **2013**, *1*, 14538-14547.

[6]   P. Friederich, V. Gómez, C. Sprau, V. Meded, T. Strunk, M. Jenne, A. Magri, F. Symalla, A. Colsmann, M. Ruben, W. Wenzel, *Adv. Mater.* **2017**, *29*, 1703505.

[7]   A. Yi, S. Chae, S. Hong, H. H. Lee, H. J. Kim, *Nanoscale.* **2018**, *10*, 21052-21061.

[8]   a) E. M. Hutter, M. C. Gélvez-Rueda, A. Osherov, V. Bulović, F. C. Grozema, S. D. Stranks, T. J. Savenije, *Nat. Mater.* **2017**, *16*, 115-120; b) T. Kirchartz, U. Rau, *J. Phys. Chem. Lett.* **2017**, *8*, 1265-1271; c) T. Wang, B. Daiber, J. M. Frost, S. A. Mann, E. C. Garnett, A. Walsh, B. Ehrler, *Energy Environ. Sci.* **2017**, *10*, 509-515.

[9]   a) S. Kitagawa, R. Kitaura, S.-i. Noro, *Angew Chem. Int. Ed.* **2004**, *43*, 2334-2375; b) H. Furukawa, K. E. Cordova, M. O'keeffe, O. M. Yaghi, *Science.* **2013**, *341*, 1230444.

[10] a) N. Keller, M. Calik, D. Sharapa, H. R. Soni, P. M. Zehetmaier, S. Rager, F. Auras, A. C. Jakowetz, A. Görling, T. Clark, T. Bein, *J. Am. Chem. Soc.* **2018**, *140*, 16544-16552; b) M. C. So, S. Jin, H.-J. Son, G. P. Wiederrecht, O. K. Farha, J. T. Hupp, *J. Am. Chem. Soc.* **2013**, *135*, 15698-15701; c) A. Aziz, A. R. Ruiz-Salvador, N. C. Hernández, S.

Calero, S. Hamad, R. Grau-Crespo, *J. Mater. Chem. A.* **2017**, *5*, 11894-11904; d) S. Yuan, T. F. Liu, D. Feng, J. Tian, K. Wang, J. Qin, Q. Zhang, Y.-P. Chen, M. Bosch, L. Zou, S. J. Teat, S. J. Dalgarno, H.-C. Zhou, *Chem. Sci.* **2015**, *6*, 3926-3930; e) M. V. Peters, R. Goddard, S. Hecht, *J. Org. Chem.* **2006**, *71*, 7846-7849; f)

[11] A structure search using the porphyrin-core in SciFinder results ~ 116,000 possible structures.

[12] a) L.-L. Li, E. W.-G. Diau, *Chem. Soc. Rev.* **2013**, *42*, 291-304; b) N. Aratani, D. Kim, A. Osuka, *Acc. Chem. Res.* **2009**, *42*, 1922-1934; c) M. Urbani, M. Grätzel, M. K. Nazeeruddin, T. Torres, *Chem. Rev.* **2014**, *114*, 12330-12396; d) A. Mahmood, J.-Y. Hu, B. Xiao, A. Tang, X. Wang, E. Zhou, *J. Mater. Chem. A.* **2018**, *6*, 16769-16797; e) S.-L. Wu, H.-P. Lu, H.-T. Yu, S.-H. Chuang, C.-L. Chiu, C.-W. Lee, E. W.-G. Diau, C.-Y. Yeh, *Energy. Environ. Sci.* **2010**, *3*, 949-955; f) M. O. Senge, Y. M. Shaker, M. Pintea, C. Ryppa, S. S. Hatscher, A. Ryan, Y. Sargeeva, *Eur. J. Org. Chem.* **2010**, 237-258; g) G. Heitmann, M. Dommaschk, R. Löw, R. Herges, *Org. Lett.* **2016**, *18*, 5228-5231.

[13] a) G. Bengasi, K. Baba, G. Frache, J. Desport, P. Gratia, K. Heinze, N. D. Boscher, *Angew. Chem. Int. Ed.* **2019**, *58*, 2103-2108; b) N. D. Boscher, M. Wang, K. K. Gleason, *J. Mater. Chem. A.* **2016**, *4*, 18144-18152; c) C. J. Medforth, Z. Wang, K. E. Martin, Y. Song, J. L. Jacobsen, J. A. Shelnutt, *Chem. Commun.* **2009**, *0*, 7261- 7277.

[14] M. Gouterman, *J. Mol. Spectr.* **1961**, *6*, 138-163.

[15] a) T. Hashimoto, Y.-K. Choe, H. Nakano, K. Hirao, *J. Phys. Chem. A.*, **1999**, *103*, 1894-1904; b) A. Rosa, G. Ricciardi, E. J. Baerends, S. J. A. van Gisbergen, *J. Phys. Chem. A*, **2001**, *105*, 3311-3327

[16] a) R. Fukuda, M. Ehara, *J. Chem. Theory. Comput.* **2013**, *9*, 470-480; b) M. Ghosh, S. Sinha, *Spectrochim. Acta. Part A: Mol. Biomol. Spectrosc.* **2015**, *150*, 959-965.

[17] a) J. Liu, C. Wöll, Chem. Soc. Rev. **2017**, 46, 5730-5770; b) H. Gliemann, C. Wöll, *Mater. Today.* **2012**, *15*, 110-116; c) O. Shekhah, J. Liu, R. A. Fischer, C. Wöll, *Chem. Soc. Rev.* **2011**, *40*, 1081-1106; d) P. Falcaro, K. Okada, T. Hara, K. Ikigaki, Y. Tokudome, A. W. Thornton, A. J. Hill, T. Williams, C. Doonan, M. Takahashi, *Nat. Mater.* **2017**, *16*, 342-348; e) S. Wannapaiboon, K. Sumida, K. Dilchert, M. Tu, S. Kitagawa, S. Furukawa, R. A. Fischer, *J. Mater. Chem. A.* **2017**, *5*, 13665-13673.

[18] J. Liu, B. Lukose, O. Shekhah, H. K. Arslan, P. Weidler, H. Gliemann, S. Bräse, S. Grosjean, A. Godt, X. Feng, K. Müllen, I.-B, Magdau, T. Heine, C. Wöll, *Sci. Rep.* **2012**, 2, 921.

[19] J. Liu, W. Zhou, J. Liu, I. Howard, G. Kilibarda, S. Schlabach, D. Couprey, M. Addicoat, S. Yoneda, Y. Tsutsui, T. Sakurai, S. Seki, Z. Wang, P. Lindemann, E. Redel, T. Heine, C. Wöll, *Angew. Chem. Int. Ed.* **2015**, *54*, 7441-7445.

[20] a) Z. Wang, J. Liu, B. Lukose, Z. Gu, P. G. Weidler, H. Gliemann, T. Heine, C. Wöll, *Nano Lett.* **2014**, *14*, 1526-1529; b) R. Haldar, M. Jakoby, A. Mazel, Q. Zhang, A. Welle, T. Mohamed, P. Krolla, W. Wenzel, S. Diring, F. Odobel, B. S. Richards, I. A. Howard, C. Wöll, *Nat. Commun.* **2018***, 9,* 4332.

Entry for the Table of Contents (Please choose one layout)

COMMUNICATION

In-silico prediction, design and fabrication of ultraviolet to near IR-absorbing porphyrin-based metal-organic thin films.
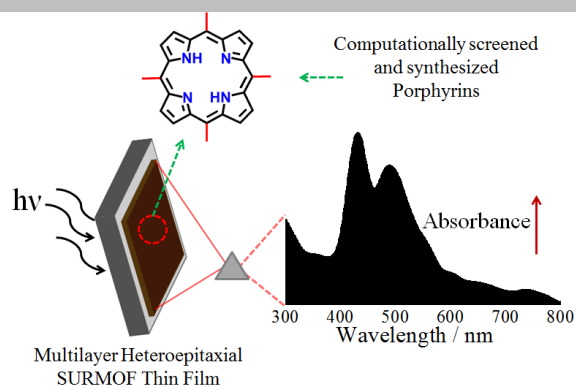
Computationally screened and synthesized Porphyrins

hν

Absorbance

Multilayer Heteroepitaxial SURMOF Thin Film

300 400 500 600 700 800
Wavelength / nm

Ritesh Haldar,[a] *Kamal Batra,*[b] *Stefan Michael Marschner,*[c] *Agnieszka B. Kuc,*[d] *Stefan Zahn,*[e] *Roland A Fischer,*[f] *Stefan Bräse,*[c,g] *Thomas Heine, **[b,d] *Christof Wöll**[a]

Page No. – Page No.

Title